

## Fowler DMO and time migration for transversely isotropic media

John Anderson\*, Tariq Alkhalifah‡, and Ilya Tsvankin‡

### ABSTRACT

The main advantage of Fowler's dip-moveout (DMO) method is the ability to perform velocity analysis along with the DMO removal. This feature of Fowler DMO becomes even more attractive in anisotropic media, where imaging methods are hampered by the difficulty in reconstructing the velocity field from surface data.

We have devised a Fowler-type DMO algorithm for transversely isotropic media using the analytic expression for normal-moveout velocity. The parameter-estimation procedure is based on the results of Alkhalifah and Tsvankin showing that in transversely isotropic media with a vertical axis of symmetry (VTI) the *P*-wave normal-moveout (NMO) velocity as a function of ray parameter can be described fully by just two coefficients: the zero-dip NMO velocity  $V_{\text{nmo}}(0)$  and the anisotropic parameter  $\eta$  ( $\eta$  reduces to the difference between Thomsen parameters  $\epsilon$  and  $\delta$  in the limit of weak anisotropy). In this extension of Fowler DMO, resam-

pling in the frequency-wavenumber domain makes it possible to obtain the values of  $V_{\text{nmo}}(0)$  and  $\eta$  by inspecting zero-offset (stacked) panels for different pairs of the two parameters. Since most of the computing time is spent on generating constant-velocity stacks, the added computational effort caused by the presence of anisotropy is relatively minor.

Synthetic and field-data examples demonstrate that the isotropic Fowler DMO technique fails to generate an accurate zero-offset section and to obtain the zero-dip NMO velocity for nonelliptical VTI models. In contrast, this anisotropic algorithm allows one to find the values of the parameters  $V_{\text{nmo}}(0)$  and  $\eta$  (sufficient to perform time migration as well) and to correct for the influence of transverse isotropy in the DMO processing. When combined with poststack *F-K* Stolt migration, this method represents a complete inversion-processing sequence capable of recovering the effective parameters of transversely isotropic media and producing migrated images for the best-fit homogeneous anisotropic model.

### INTRODUCTION

Fowler's (1984 and 1988) dip-moveout (DMO) algorithm is traditionally used for prestack velocity analysis in isotropic media [for a concise overview of the method also see Hale (1991)]. The main advantage of the Fowler algorithm is the ability to generate a large number of stacked (zero-offset) sections covering a wide range of stacking velocities. These sections can then be migrated using Stolt's *F-K* poststack migration operator. The combination of Fowler DMO with Stolt poststack migration is usually called Fowler prestack time migration; however, if the velocity analysis has already been performed, other methods are usually more efficient in imaging the data.

Fowler prestack time migration is often used when an interpreter wants to efficiently generate a large number of

constant-velocity, prestack-time-migration displays to get a feel for what possible structures could be imaged with more sophisticated techniques. The multiple constant-velocity-migration panels bring pieces of complicated structure into focus, allowing for an early rough interpretation, which is especially valuable in new exploration areas. Also, since out-of-plane events typically image on a 2-D migration at velocities different from the true medium velocities, they can sometimes be identified through the interplay of image quality and migration velocity.

On the whole, Fowler DMO is designed more for parameter estimation and preliminary interpretation than for final imaging. More elaborate depth-migration methods usually are required to obtain accurate depth images of complicated structures. The migration-velocity-analysis panels produced by

Presented at the 64th Annual International Meeting, Society of Exploration Geophysicists. Manuscript received by the Editor December 20, 1994; revised manuscript received August 21, 1995.  
 \*Mobil E & P Technical Center, Room 10D65, 3000 Pegasus Drive, Dallas, TX 75247.  
 ‡Center for Wave Phenomena, Colorado School of Mines, Golden, CO 80401.  
 © 1996 Society of Exploration Geophysicists. All rights reserved.

the Fowler algorithm can be used in the same manner as conventional constant-velocity-stack panels to estimate the normal moveout (NMO) velocity for horizontal reflectors. In isotropic media, the zero-dip NMO velocity on short spreads is equal to the rms vertical velocity and, therefore, can be inverted for the interval velocities using the Dix formula. A definite advantage of the migration panels produced in the Fowler DMO process is that the velocities have been dip-corrected; also, the spatial positions of reflectors are less distorted than on constant-velocity-stack panels.

Here, we show that the advantages of the Fowler dip-moveout method can be exploited fully in transversely isotropic media with a vertical axis of symmetry (VTI) by combining it with the analytic solution for NMO velocity given in Tsvankin (1995). Our extension of Fowler DMO to VTI media involves a search for two effective parameters of VTI media that replace a single parameter (velocity) in isotropic media. We discuss two ways to make this search comparable in efficiency to the velocity scan in the isotropic Fowler method and demonstrate the performance of the new algorithm on synthetic examples and field data. To produce a migrated image, we combine Fowler DMO with Stolt's (1978) poststack frequency-wavenumber ( $F$ - $K$ ) migration adapted for transverse isotropy.

## ANALYTIC FORMULATION

### Fowler DMO in isotropic media

The first step of the Fowler DMO process is the generation of common-midpoint stacked panels for a range of stacking velocities. Horizontal and dipping events stack coherently on different velocity panels, thus "splitting" subsurface structures into pieces containing different dips. The goal of Fowler DMO is to collect all horizontal and dipping events on the panel corresponding to the correct value of the zero-dip NMO velocity  $V_{\text{nmo}}(0)$ .

The original implementation of Fowler DMO (Fowler, 1984, 1988) is based on the dip-dependence of NMO velocity valid for homogeneous, isotropic media (Levin, 1971):

$$V_{\text{nmo}}(\phi) = \frac{V_{\text{nmo}}(0)}{\cos \phi} = \frac{V_{\text{nmo}}(0)}{\sqrt{1 - p^2 V_{\text{nmo}}^2(0)}}, \quad (1)$$

where  $p = \sin \phi / V$  is the ray parameter, which can be represented in the frequency-wavenumber domain as

$$p = \frac{1}{2} \frac{dt_0}{dy} = \frac{k}{2\omega_0}. \quad (2)$$

Here  $t_0(y)$  is the two-way time on the zero-offset (or stacked) section,  $y$  is the midpoint location,  $k$  is the horizontal wavenumber corresponding to  $y$ , and  $\omega_0$  is the angular frequency corresponding to  $t_0$ .

The output panel for a given  $V_{\text{nmo}}(0)$  is built by obtaining the dip-dependent velocity  $V_{\text{nmo}}$  as a function of the ray parameter  $p$  [using equation (1)] and transferring the events from the panel corresponding to  $V_{\text{nmo}}(p)$  to the panel for  $V_{\text{nmo}}(0)$ . This operation is carried out in the frequency-wavenumber ( $\omega - k$ ) domain, where the ray parameter is given by equation (2). The resampling procedure is repeated for a range of zero-dip NMO (stacking) velocities to find the

value of  $V_{\text{nmo}}(0)$  that coherently stacks both horizontal and dipping reflectors.

Once the panel corresponding to the best-fit velocity  $V_{\text{nmo}}(0)$  has been identified, the data are corrected for dip moveout and made ready for poststack frequency-wavenumber migration. While this approach is not recommended if the parameters of the medium are well-known or if only one constant-velocity, prestack time-migration panel is desired, it can be efficiently used in velocity analysis. A somewhat crude final variable-velocity migration can be "painted" or interpolated from the multiple constant-velocity-migration panels if the velocity increment between the output panels is fine enough to avoid aliasing.

In practical terms, the traditional isotropic Fowler DMO algorithm combined with Stolt poststack migration requires on the order of 100 constant-velocity stacks of the input data, usually computed in constant increments of the squared slowness. Then these constant-velocity stacks are Fourier-transformed to the frequency-wavenumber domain and, for each frequency-wavenumber component, the data are resampled from stacking velocity to a set of reference DMO (true medium) velocities. Finally, the data are migrated by resampling from DMO frequency to migration frequency via the Stolt  $F$ - $K$  algorithm.

### Fowler DMO for transverse isotropy

Our goal here is to extend the methodology of Fowler DMO to transversely isotropic media. If the medium above the reflector is anisotropic, equation (1) becomes inaccurate and should be replaced by the following expression derived by Tsvankin (1995):

$$V_{\text{nmo}}(\phi) = \frac{V(\phi)}{\cos \phi} \frac{\sqrt{1 + \frac{1}{V(\phi)} \frac{d^2 V}{d\theta^2}}}{1 - \frac{\tan \phi}{V(\phi)} \frac{dV}{d\theta}}, \quad (3)$$

where  $V(\theta)$  is the phase velocity as a function of the phase angle; the derivatives should be evaluated at the dip angle  $\phi$ .

Equation (3) is valid for all wave types (except for converted waves) in symmetry planes of any anisotropic homogeneous medium; here, however, we will use it only for quasi- $P$ -waves in VTI media (the qualifier "quasi" will be omitted hereafter). Anderson and Tsvankin (1994) showed that the same equation can be used to perform DMO by Fourier transform in symmetry planes of arbitrary anisotropic media.

$P$ -wave propagation can be described by the vertical  $P$ - and  $S$ -wave velocities  $V_{P0}$  and  $V_{S0}$  and two dimensionless anisotropic parameters  $\epsilon$  and  $\delta$  (Thomsen, 1986). As discussed in an overview paper by Tsvankin (1996), Thomsen parameters are convenient to use in TI media with any magnitude of velocity variations and not just for weak anisotropy. The velocity  $V_{S0}$  has only a small influence on  $P$ -wave NMO velocity and, for practical purposes of seismic inversion and processing, can be ignored (Tsvankin, 1995, 1996). Since here we concentrate on  $P$ -wave propagation, we limit ourselves to a single  $V_{P0}/V_{S0}$  ratio for all output velocity panels.

To be applied in our anisotropic DMO algorithm, the NMO velocity [equation (3)] should be expressed through the ray parameter  $p$  rather than the dip angle. Although the basic relation between the reflection slope on the zero-offset section

and  $p$  in equation (2) remains valid in anisotropic media, the ray parameter becomes a more complicated function of the dip angle and anisotropic coefficients:  $p = \sin \phi / V(\phi)$ . However, the NMO velocity equation (3) can be calculated through the ray parameter in a straightforward way (e.g., parametrically) using the phase-velocity equations for transverse isotropy.

The main complication in implementing a Fowler-type DMO process using equation (3) is the difficulty in dealing with three independent parameters ( $V_{p0}$ ,  $\epsilon$ , and  $\delta$ ) instead of just one scalar velocity in isotropic models. Fortunately, Alkhalifah and Tsvankin (1995) found that in VTI media, the  $P$ -wave NMO velocity as a function of the ray parameter is entirely controlled by just two combinations of these coefficients: the NMO velocity for a horizontal reflector  $V_{nmo}(0)$  and the effective parameter  $\eta$ :

$$V_{nmo}(0) = V_{p0} \sqrt{1 + 2\delta}, \quad (4)$$

$$\eta = \frac{\epsilon - \delta}{1 + 2\delta}. \quad (5)$$

Note that  $\eta$  vanishes not only for pure isotropy ( $\epsilon = \delta = 0$ ), but also in any elliptically anisotropic media ( $\epsilon = \delta$ ). While reflection moveout in homogeneous elliptically anisotropic media is hyperbolic (e.g., Helbig, 1983; Dellinger, 1991), moveout velocity for horizontal reflectors, as well as the dependence of NMO velocity on the reflector dip, are distorted by anisotropy (Uren et al., 1990; Tsvankin, 1995). Nonetheless, elliptical anisotropy is equivalent to isotropy in Fowler DMO processing because the dependence of the NMO velocity on the ray parameter is exactly the same as in isotropic media (Alkhalifah and Tsvankin, 1995). Although the isotropic Fowler method remains valid for elliptically anisotropic media, the reference velocity is no longer equal to the true vertical velocity. For elliptical anisotropy, the resampling procedure makes it possible to recover the zero-dip NMO velocity  $V_{nmo}(0)$ , which is equal to the horizontal velocity, and not the velocity appropriate for depth conversion. However, the elliptical model cannot be considered as typical for subsurface formations (Thomsen, 1986).

For nonelliptical VTI media, knowledge of  $V_{nmo}(0)$  and  $\eta$  is sufficient not only to build the  $P$ -wave NMO velocity as a function of the ray parameter, but also to perform all essential time-related processing steps including poststack and prestack time migration (Alkhalifah and Tsvankin, 1995). The vertical velocity  $V_{p0}$ , however, is necessary for accurate depth migration or time-to-depth conversion.

Alkhalifah and Tsvankin (1995) have also shown that  $V_{nmo}(0)$  and  $\eta$  can be recovered from the  $P$ -wave NMO velocities and the corresponding ray parameters (reflection slopes) for two distinctly different dips. Here, we suggest a practical way to include the parameter-estimation step into the processing sequence via a Fowler-type velocity analysis. Indeed, the idea of the isotropic Fowler algorithm is to use relation (1) between NMO velocities for a horizontal and dipping reflector to find the zero-dip NMO velocity that allows proper imaging of all horizontal and dipping events. Likewise, we can use the analytic NMO equation for anisotropic media (3) to find the pair of values  $[V_{nmo}(0), \eta]$  that would produce the best zero-offset (stacked) section after resampling in the  $\omega - k$  domain. This implies that we have to replace a 1-D search for the true medium velocity in the isotropic Fowler

algorithm by a 2-D search in transversely isotropic media. However, since most of the computing time in Fowler DMO is spent on generating constant-velocity stacks, a more complicated resampling procedure hardly increases the overall computational cost.

Also, there are two ways to facilitate this search and to make the process of choosing the best-fit anisotropic parameters more efficient. First, we can use the constant-velocity stacks produced at the initial stage of the Fowler DMO process to pick the stacking velocities and ray parameters for two different dips (e.g., for a horizontal and dipping reflector). These data are sufficient to invert for  $V_{nmo}(0)$  and  $\eta$  using the numerical technique developed in Alkhalifah and Tsvankin (1995). This preliminary estimate allows us to reduce the range of both parameters in the 2-D search described above.

Second, the NMO velocity for horizontal reflectors  $V_{nmo}(0)$  can be obtained by the conventional NMO velocity analysis performed before DMO processing. In this case, the velocity analysis in Fowler DMO becomes one-dimensional, as in isotropic media. However, for transverse isotropy the parameter to be determined is the effective coefficient  $\eta$  rather than the zero-dip NMO velocity in the isotropic algorithm. As mentioned above, the processing sequence comprising NMO velocity analysis and Fowler DMO is not considered to be efficient in isotropic media because there is no need to produce multiple velocity panels after the velocity has been determined. The situation in transversely isotropic media is entirely different because of the presence of an additional independent parameter. Even if the zero-dip, normal-moveout velocity has been obtained from NMO velocity analysis, Fowler DMO represents a practical way to recover the second parameter ( $\eta$ ) and, at the same time, perform the DMO correction.

To migrate DMO-corrected stacked panels, we extend the isotropic Stolt (1978)  $F$ - $K$  migration algorithm to VTI media. The only substantial change required in the Stolt method is the replacement of the isotropic velocity by the dip-dependent phase-velocity function for transversely isotropic media (Kitchenside, 1991). We use a reference velocity equal to  $V_{p0}$  for defining our time-migration depth step and note that

$$\frac{V_{p0}k}{2\omega_m} = \tan \phi, \quad (6)$$

and

$$\omega_0 = \omega_m \frac{V(\phi)}{V_{p0}} \sqrt{1 + \frac{V_{p0}^2 k^2}{4\omega_m^2}} = \frac{\omega_m}{\cos \phi} \frac{V(\phi)}{V_{p0}}. \quad (7)$$

Here,  $\omega_0$  is the zero-offset angular frequency after DMO but before migration,  $\omega_m$  is the angular frequency after migration, and  $\phi$  is the dip angle associated with the reflector of interest. The rest of the Stolt's isotropic algorithm remains essentially unchanged. Note that equation (7) reduces to the isotropic cosine-of-dip Stolt relationship if  $V(\phi)$  equals  $V_{p0}$ .

In the current version of the Fowler algorithm, we choose a set of reference values for  $V_{nmo}(0)$  and  $\eta$  and output either dip-moveout corrected stacks or full time migrations for a number of pairs of the two parameters. The displays of these panels are visually inspected to determine the pair  $[V_{nmo}(0), \eta]$  that best images events over a wide range of dips.

Similar to the Hale-type DMO method in Anderson and Tsvankin (1994), this extension of Fowler DMO is based on the

hyperbolic moveout equation and, therefore, cannot correct for nonhyperbolic moveout on long spreads. However, in agreement with the results in Anderson and Tsvankin (1994) and Tsvankin (1995), nonhyperbolic moveout in VTI media turns out to be less significant (for a fixed spreadlength-to-depth ratio) for steep dips than for horizontal events. Therefore, for typical VTI media, NMO correction is more hampered by deviations from hyperbolic moveout than is DMO removal. In fact, since the moveout for steep dips is so close to hyperbolic, and the anisotropic DMO method uses the correct dip-dependent NMO velocity, we can expect that our algorithm will make it possible to align dipping reflections even at fairly large offsets.

### NUMERICAL IMPLEMENTATION

The numerical implementation follows the analytic description closely. The constant-velocity stacks are computed in constant increments of slowness-squared from zero (corresponding to infinite velocity) to a predefined value of  $1/V_{\min}^2$  at a fairly fine increment. The initial mute time on the far offsets needs to obey

$$t_{\text{mute}} \geq F_{\max} x^2 \Delta q \quad (8)$$

to avoid aliasing during the resampling over stacking velocity for DMO in the slowness-squared, frequency-wavenumber domain. Here  $F_{\max}$  is the maximum frequency in the data,  $x$  is the source-receiver offset, and  $\Delta q$  represents the increment in the squared slowness used to generate the constant-velocity stacks.

The DMO step requires resampling from the dip-dependent stacking velocity to the zero-dip NMO velocity  $V_{\text{nmo}}(0)$  based on equation (3). Since  $V_{\text{nmo}}(0)$  does not depend on the dip angle, it can be called the "DMO" velocity (Fowler, 1988). To aid in the efficiency in this step, we tabulate NMO velocity as a function of the ray parameter. For each desired output reference velocity  $V_{\text{nmo}}(0)$  and the parameter  $\eta$ , we calculate  $V_{\text{nmo}}$  and  $p$  [ $p = \sin \phi / V_P(\phi)$ ] as functions of the dip  $\phi$ . Then we create a table  $V_{\text{nmo}}(p)$  and interpolate it to one whose abscissa is in constant increments of  $p$ . Fowler DMO is accomplished by looking up the appropriate value of the stacking velocity  $V_{\text{nmo}}(p)$  in the table for a given  $p = k/(2\omega_0)$  and resampling the data from the stacking velocity to the DMO velocity  $V_{\text{nmo}}(0)$  in the frequency-wavenumber domain.

The VTI Stolt time migration step requires resampling data from DMO frequency to migration frequency. Once again, we build tables to help with efficiency. First, we assume a certain value for the vertical velocity  $V_{P0}$ . For each desired output  $V_{P0}$  and  $\eta$ , we first loop over angles from  $0^\circ$  to  $89^\circ$  and table an abscissa of  $\tan \phi / V_{P0}$  associated with an ordinate of  $V_P(\phi) / (V_{P0} \cos \phi)$ . Then, we interpolate that table to one whose abscissa is in even increments of  $\tan \phi / V_{P0}$ . Stolt migration is carried out by looking up in the table the appropriate frequency scaling factor for each abscissa of  $(V_{P0}k)/(2\omega_m)$  and resampling from DMO to migration frequency.

Note that it is not necessary to know the vertical velocity  $V_{P0}$  in DMO or time migration. Knowledge of  $V_{P0}$  is critical for depth conversion or depth migration, but an inaccurate value of  $V_{P0}$  in DMO or time migration does not influence the quality of reflector imaging as long as the truly relevant parameters,  $V_{\text{nmo}}(0)$  and  $\eta$ , are correct (Alkhalifah and Tsvankin, 1995). While building phase velocity tables as a

function of the ray parameter, a typical choice for  $V_{P0}$  would be  $V_{P0} = V_{\text{nmo}}(0)$  ( $\delta = 0$ ), but an infinite number of other choices are equally valid. Also, we assume a constant value of  $V_{S0}/V_{P0} = 0.5$  since the dependence of  $P$ -wave NMO velocity on  $V_{S0}$  can be ignored.

The volume of data generated during the computation of constant-velocity stacks can be very large for practical-size problems. This implementation uses a set of block-matrix transpose routines that allow the disk files to span multiple disks and require minimal RAM memory. The block-matrix transpose code allows the data to be accessed in constant slices of time, velocity, or midpoint, as needed at various stages of the algorithm. The resampling operations required for both DMO and migration are done with 8-point sinc function interpolators tabled to be accurate to within 1/512 of a sample point.

### SYNTHETIC EXAMPLE

We tested the Fowler algorithm on a homogeneous VTI model with  $V_{\text{nmo}}(0) = 3 \text{ km/s}$  and  $\eta = 0.15$  ( $V_{P0} = 2860 \text{ m/s}$ ,  $\epsilon = 0.215$ ,  $\delta = 0.05$ ) shown in Figure 1. The range of dips in the model (from  $0^\circ$  to  $75^\circ$ ) allows us to thoroughly examine the performance of the algorithm. A Ricker wavelet with a peak frequency of 20 Hz was convolved with the synthetic data computed by anisotropic ray tracing (Alkhalifah, 1995). A total of 601 midpoint locations were recorded with a trace spacing of 25 m and a listen time of 8 s; the displays will show only a 1.75 s window of data at the location of the target reflectors. The horizontal and temporal apertures recorded are barely sufficient to image the  $75^\circ$  reflector with some smearing.

The full Fowler prestack migration (Fowler DMO and Stolt poststack migration) was applied to 61-fold prestack synthetic data from this model for offsets ranging from 0 to 3000 m in 50-m increments. We used six reference velocities  $V_{\text{nmo}}(0)$  and six reference values of  $\eta$ , yielding a total of 36 output constant-velocity, prestack-time-migration panels. The velocity  $V_{\text{nmo}}(0)$  was changed from 2700 m/s to 3450 m/s in steps of 150 m/s (or from 10% too low to 15% too high in 5% increments of the correct value). The parameter  $\eta$  was allowed to vary over a fairly wide range from 0.0 to 0.25 in steps of 0.05.

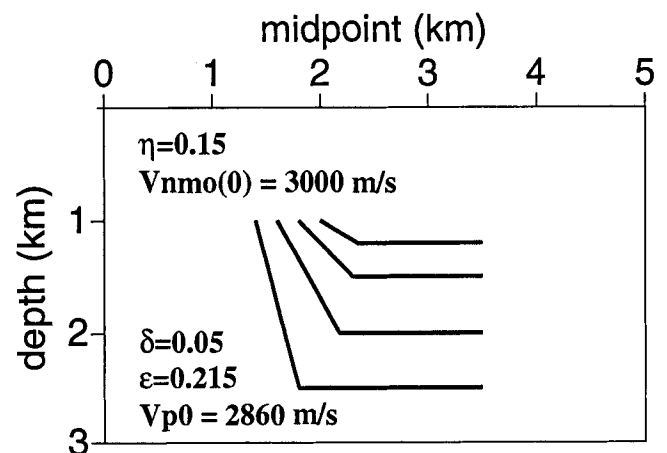


FIG. 1. Synthetic data from this model, generated by ray tracing, were used to test the Fowler algorithm. The dip angles are  $30^\circ$ ,  $45^\circ$ ,  $60^\circ$ , and  $75^\circ$ .

A subset of the output panels is displayed in Figures 2–4 in a compressed format to compare the performance of the DMO-migration sequence for different pairs of  $V_{\text{nmo}}(0)$  and  $\eta$ . Figures 2–4 have been plotted with the same gain to allow comparisons of amplitudes between the different panels. Figure 2 shows multiple  $\eta$  panels for the correct value of  $V_{\text{nmo}}(0)$ . The dipping events appear undermigrated on the lower  $\eta$  panels and overmigrated on the higher  $\eta$  panels; also, poor focusing of the dipping events for the wrong values of  $\eta$  is evident. Since for a fixed  $V_{\text{nmo}}(0)$ , an increase in the parameter  $\eta$  leads to a higher horizontal velocity, errors in  $\eta$  can be related to undermigration and overmigration in the same way as errors in migration velocity in isotropic imaging (Alkhalifah and Tsvankin, 1995). The best image occurs for the

correct value of  $\eta = 0.15$  [Figure 2(d)]; some smearing on the  $75^\circ$  event is caused by the limited spatial and temporal aperture of the data used in this test.

Figure 3 shows multiple migration velocities  $V_{\text{nmo}}(0)$  for the correct value of  $\eta$ . As expected, the best image is obtained for the correct velocity of 3000 m/s in Figure 3(c). It is interesting to mention that during a different set of tests in which we kept the largest offsets without using a reasonable mute (not shown here), the two earliest horizontal reflections were imaged best on a 200 m/s-faster panel, and the third horizontal event appeared to focus best on a panel with a 100 m/s faster velocity. We believe this was because of the influence of nonhyperbolic moveout on the stacking velocity (Tsvankin and Thomsen, 1994). A mute more typical of that used on real data cured this

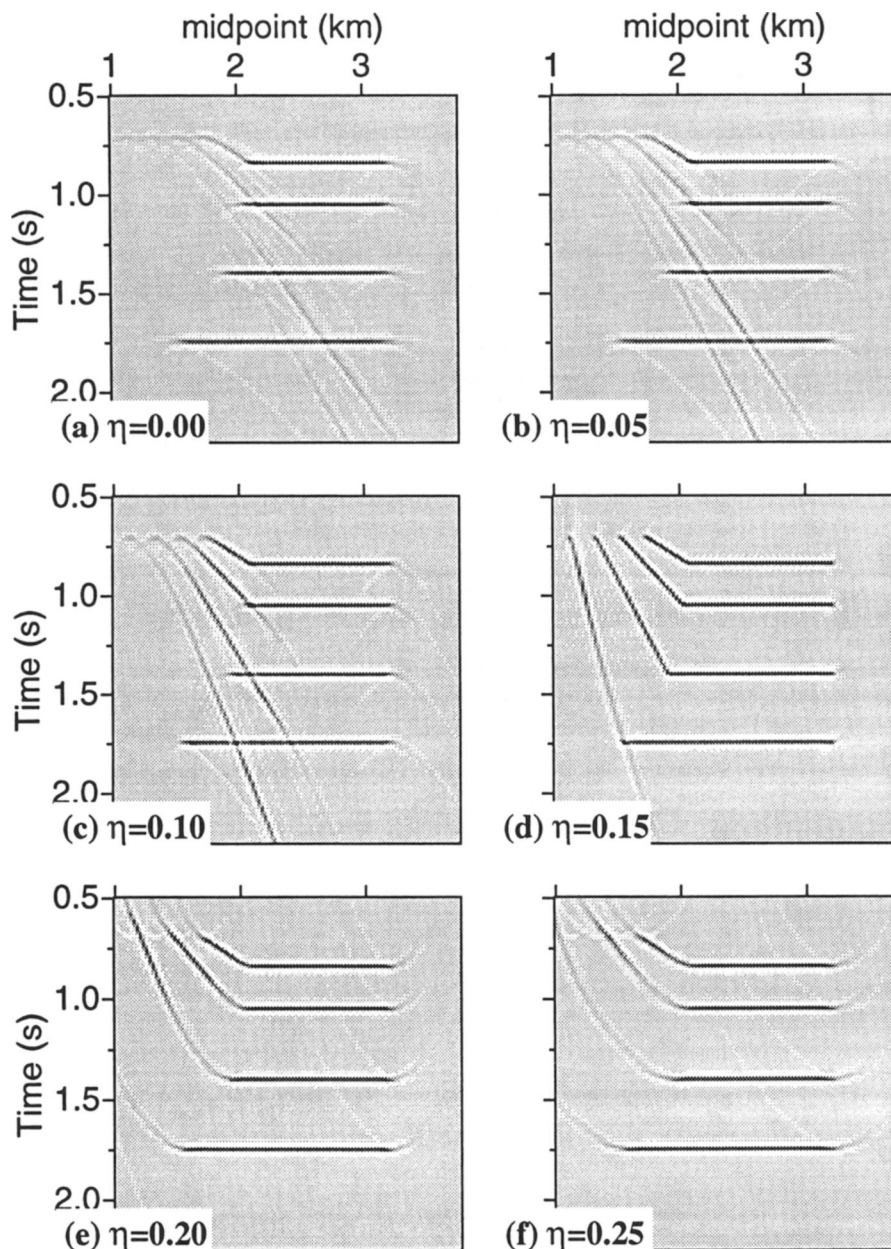


FIG. 2. Output Fowler DMO/Stolt migration stacked panels for the correct  $V_{\text{nmo}}(0) = 3000$  m/s and different values of  $\eta$ . Panel (d) corresponds to the correct model parameters.

problem. The moveout from the deeper reflectors and the dipping events is closer to hyperbolic and focuses best on the correct panel, even if all offsets are included.

Figure 4 shows multiple migration velocities for  $\eta = 0$ , duplicating the results of the isotropic (or elliptically anisotropic) algorithm. It is possible to get a fairly good image of most dipping events by using a velocity that is faster than the correct one (see Figure 4f), but at this faster velocity the horizontal events go out of focus. Therefore, the conventional Fowler DMO method cannot handle nonelliptical transversely isotropic models.

As a whole, the best-quality image by far is obtained by using the correct velocity and correct value for  $\eta$ . This is encouraging, as there needs to be a significant difference in image

quality for an interpreter to be able to pick the correct value of  $\eta$ . One can obtain acceptable images for an erroneous pair  $[\eta, V_{\text{nmo}}(0)]$ , but for only a limited range of dips. For instance, if we use a smaller  $V_{\text{nmo}}(0)$ , we can focus a given dipping event by using a higher value of  $\eta$ ; however, in this case horizontal events cannot be imaged well because the stacking velocity for them is too low.

Note that this example verifies the Alkhalifah and Tsvankin (1995) result that only  $V_{\text{nmo}}(0)$  and  $\eta$  are required for time-domain processing. Internally, in our code, the algorithm sets the vertical velocity equal to  $V_{\text{nmo}}(0)$ ,  $\delta = 0$ , and  $\epsilon = \eta$ . Those are not the true Thomsen medium parameters for the model as described in Figure 1. However, we have used the correct values of  $V_{\text{nmo}}(0)$  and  $\eta$  for our DMO-time migration test, and

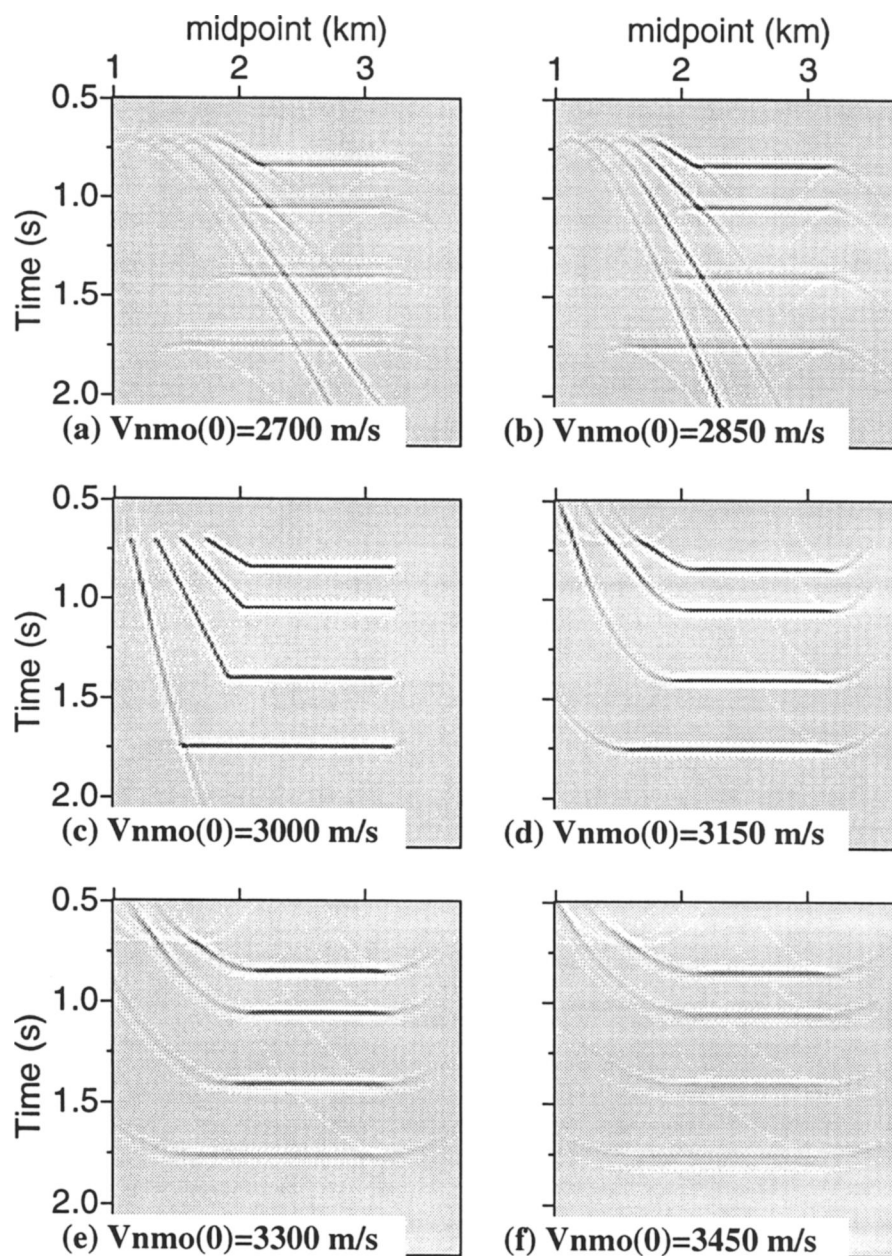


FIG. 3. Fowler DMO/Stolt migration stacked panels for the correct  $\eta = 0.15$  and different values of  $V_{\text{nmo}}(0)$ . Panel (c) corresponds to the correct model parameters.

therefore obtained an accurate image. With these choices for mapping  $V_{\text{nmo}}(0)$  and  $\eta$  to Thomsen's parameters, we ensure that our anisotropic images temporally tie those generated by isotropic codes. Another choice of the vertical velocity rescales the time axis without influencing the quality of imaging.

The cost associated with the anisotropic algorithm is almost identical to that of the isotropic method for a given number of output panels. It should be emphasized that we could have calculated several hundred output migration panels at an increase in computational effort of only about 20% because most of the computational time goes into the generation of the constant-velocity stacks needed for the DMO resampling step. The real limitation becomes disk space, input/output, and the resources required for displaying all of the output panels.

#### OFFSHORE AFRICA EXAMPLE

We applied the anisotropic Fowler algorithm to a field data set from offshore Africa provided to the Center for Wave Phenomena by Chevron Overseas Petroleum, Inc. Our goal was to image the reflectors associated with fault planes beneath a thick anisotropic shale sequence. The dip angle of the fault in Figure 5 is about  $40^\circ$ , while the subhorizontal events dip at less than  $5^\circ$ .

The data have a vertical velocity gradient of about  $0.6\text{--}0.7\text{ s}^{-1}$  that our Fowler algorithm, designed for homogeneous media, cannot honor precisely. We accounted for the gradient approximately by interpolating (painting) a final output section using panels with different  $V_{\text{nmo}}(0)$  and  $\eta$  at different vertical times

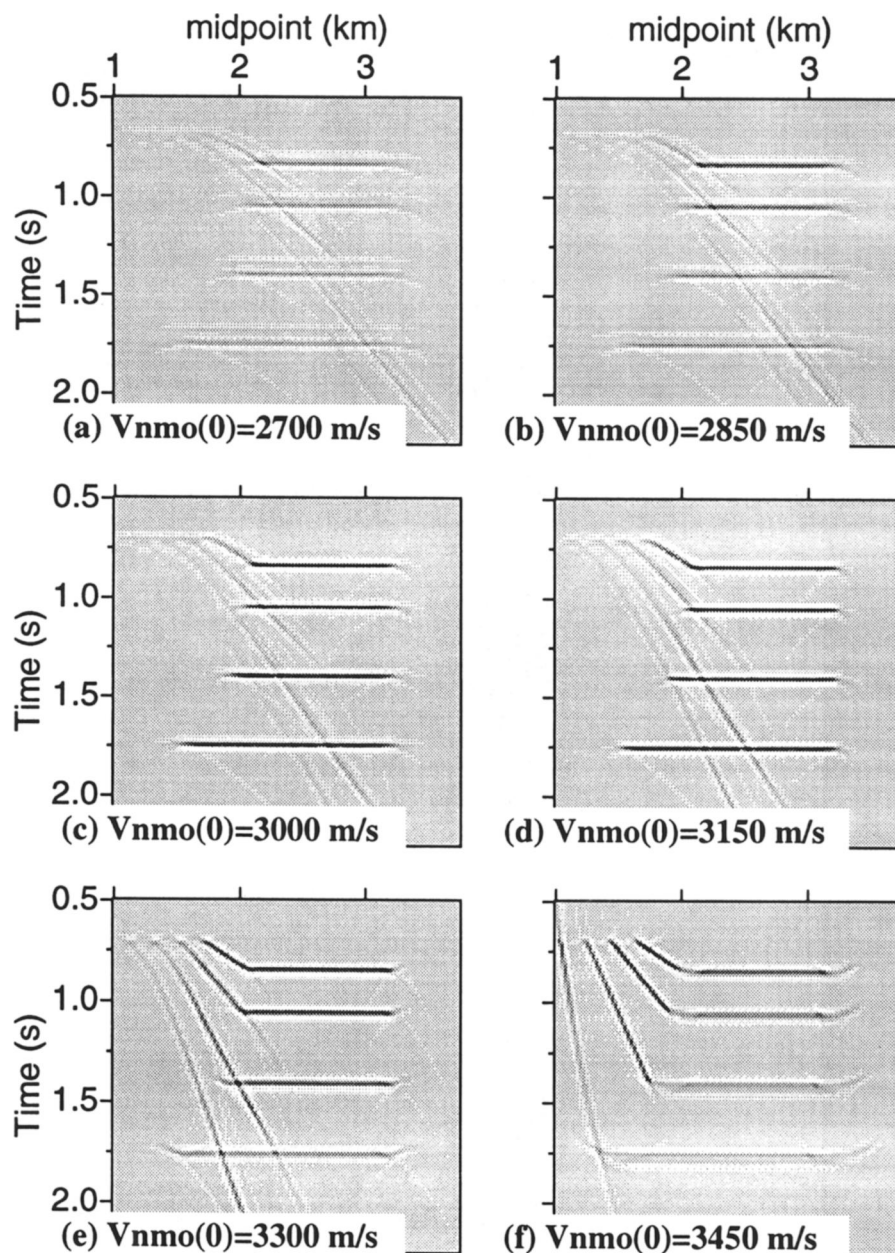


FIG. 4. Fowler DMO/Stolt migration stacked panels generated by the isotropic algorithm ( $\eta = 0$ ).

$t_0$  and spatial locations (i.e., we interpolated between triplets  $[V_{\text{nmo}}(0), \eta, t_0]$  specified at each spatial location). Therefore, although the algorithm worked with a homogeneous model, the parameters of the output section  $[V_{\text{nmo}}(0)$  and  $\eta]$  vary in time and space. In the building of the final image, we used a time-dependent value of  $V_{\text{nmo}}(0)$  obtained by the conventional velocity analysis and scanned just for the best-fit parameter  $\eta$ .

In Figure 5, six DMO-corrected stacked panels are displayed for values of  $\eta$  ranging from 0 to 0.20. On each panel,  $V_{\text{nmo}}(0)$  is a function of time as determined from NMO velocity (semblance) analysis, while  $\eta$  is kept constant. A component of the fault plane reflector appears in its unmigrated position somewhere near 1.8 s at about midpoint 850. The best image of this DMO-corrected fault-plane reflection occurs at an  $\eta$  value between 0.08 and 0.12. Figure 6 shows the equivalent results

obtained by applying the full Fowler DMO-Stolt migration algorithm for the same range of  $\eta$ . Interestingly, the best fault-plane image in the migrated position of 1.5 s at midpoint 950 appears for an  $\eta$  value between 0.12 and 0.16. It should be emphasized that the anisotropic DMO-migration sequence provides a much clearer image of the fault plane reflection than that obtained by the isotropic algorithm on the panel corresponding to  $\eta = 0$ .

The discrepancy between the  $\eta$  values estimated by DMO versus DMO plus migration is most likely caused by the influence of the velocity gradient and, possibly, by a vertical gradient in  $\eta$ . An increasing vertical velocity tends to “squeeze” the desired inhomogeneous DMO operator (Hale and Artley, 1993). Our homogeneous DMO  $\eta$  scan will adapt to the gradient by underestimating the true value of  $\eta$

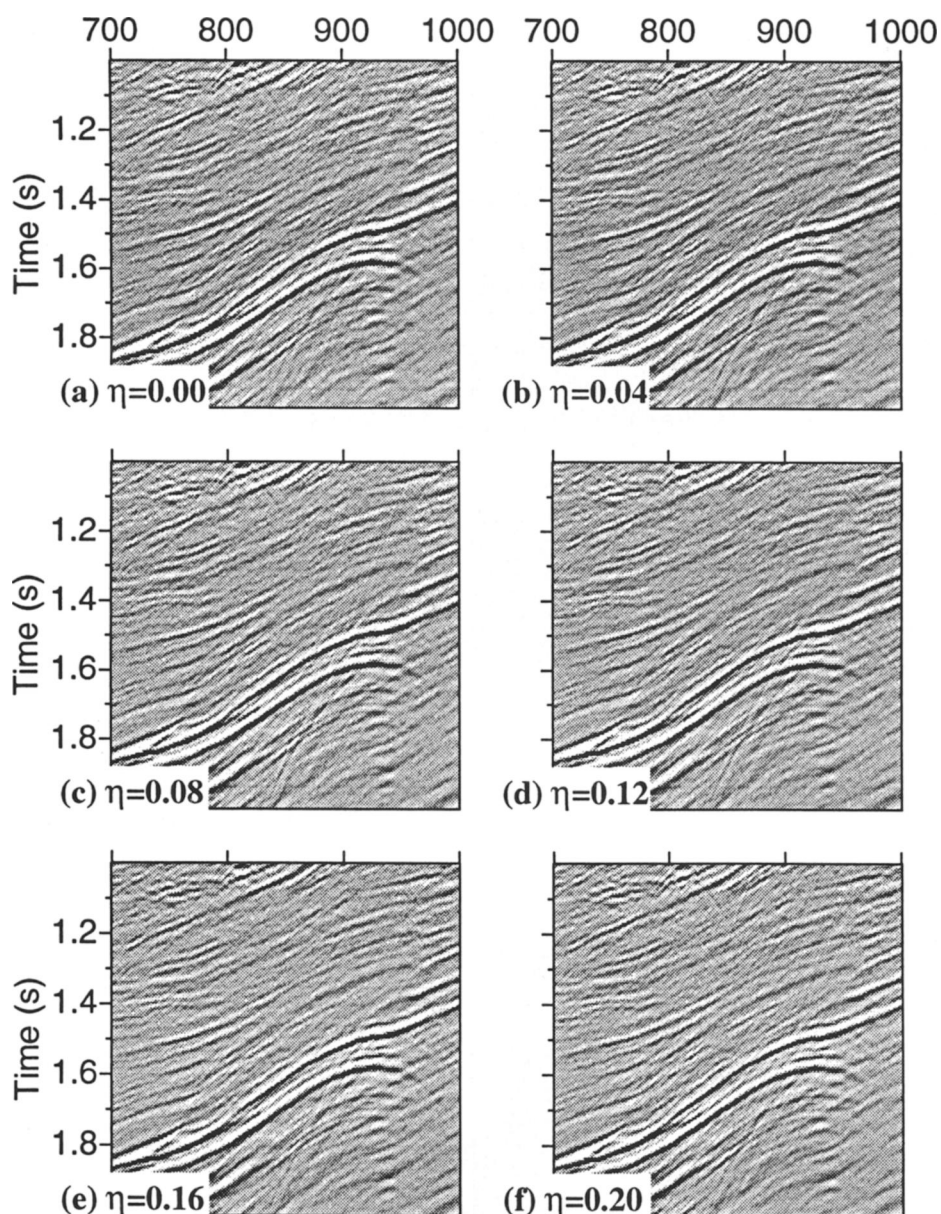


FIG. 5. Fowler DMO panels of the field data set for different values of  $\eta$ . Each panel is interpolated (painted) using a time-dependent velocity function  $V_{\text{nmo}}(0)$ .



(Tsvankin, 1995). In contrast, that same vertical velocity gradient will tend to “broaden” the desired inhomogeneous migration operator causing our homogeneous algorithm to adapt by overestimating  $\eta$  during the migration step. The fault-plane event migrates from about midpoint 850 and time 1.95 s on the DMO section (Figure 5) to its final location at midpoint 950 and time 1.5 s on the migrated section (Figure 6). It tends to migrate further horizontally for larger values of  $\eta$ ; we also noticed that the deeper events on the DMO  $\eta$  scan (not shown) do image better at higher values of  $\eta$ .

The trade-off between the parameter  $\eta$  and vertical velocity gradient allows our algorithm to construct fairly good DMO images of fault planes, even in vertically inhomogeneous media. This suggests that an appropriate use of our method may be to obtain a DMO stacked section that preserves

fault-plane reflections and migrate it by a more sophisticated  $V(z)$  anisotropic algorithm. Ultimately, however, it is clear that an even better job of imaging and  $\eta$  estimation could be done with an approach that makes it possible to account for both anisotropy and inhomogeneity (Alkhalifah and Tsvankin, 1995).

#### DISCUSSION AND CONCLUSIONS

We have presented an extension of the Fowler DMO and Stolt poststack time-migration algorithms to transversely isotropic media with a vertical symmetry axis (VTI). The idea of the conventional Fowler DMO is to combine dipping and horizontal events, stacked at different velocities, on a single section corresponding to the true zero-dip NMO velocity. In isotropic media, the Fowler method is implemented by resam-

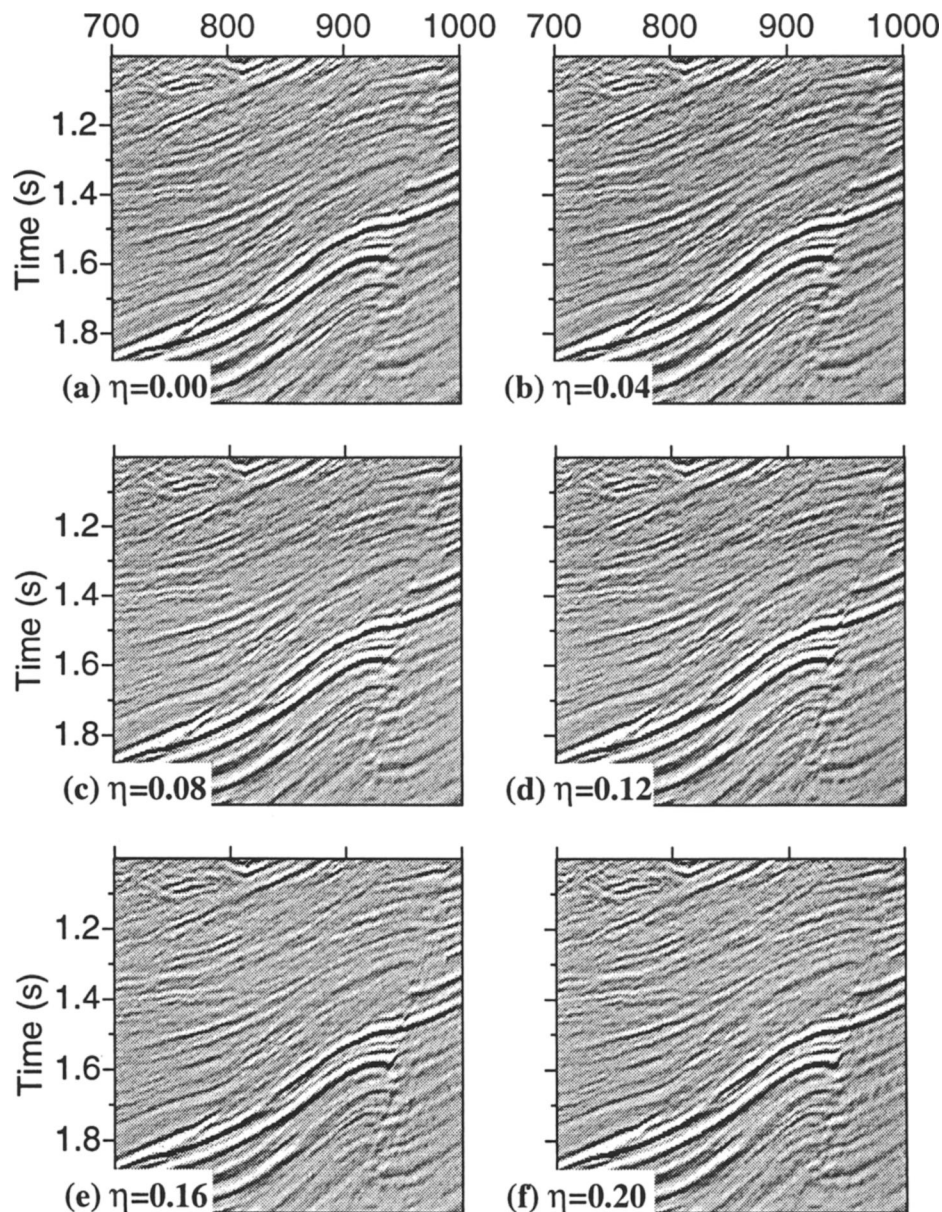


FIG. 6. Fowler DMO/Stolt migration panels of the field data set for different values of  $\eta$ . Each panel is painted using a time-dependent velocity function  $V_{\text{nmo}}(0)$ .

pling in the frequency-wavenumber domain using the cosine-of-dip dependence of the stacking velocity. In VTI media, we accomplish the same goal by applying the analytic equation for the normal-moveout velocity for dipping reflectors given by Tsvankin (1995).

The importance of Fowler DMO as a velocity-analysis tool is much more significant in VTI media, where the  $P$ -wave NMO velocity depends on two effective parameters, the zero-dip velocity  $V_{\text{nmo}}(0)$  and the anisotropic parameter  $\eta = (\epsilon - \delta)/(1 + 2\delta)$  (Alkhalifah and Tsvankin, 1995). These two parameters are sufficient to carry out all essential time-processing steps, including dip moveout and prestack and poststack time migration. Fowler DMO modified for VTI media represents a practical way of obtaining the values of  $V_{\text{nmo}}(0)$  and  $\eta$  in the process of DMO correction. Although the anisotropic Fowler DMO algorithm requires a 2-D scan over  $V_{\text{nmo}}(0)$  and  $\eta$ , the total computational cost does not increase significantly because most of the computing time is spent on generating constant-velocity stacks at the first stage of DMO processing. Thus, Fowler DMO provides an opportunity to carry out parameter estimation and, at the same time, perform the DMO correction.

Also, we suggest two alternative ways to simplify the 2-D estimation procedure in the anisotropic Fowler algorithm. First, the velocity analysis in Fowler DMO can be restricted to a single parameter ( $\eta$ ) by obtaining the NMO velocity for horizontal reflectors  $V_{\text{nmo}}(0)$  from conventional NMO velocity analysis. Second, the constant-velocity stacks produced at the initial stage of the Fowler DMO process are ideally suited to perform the inversion for  $V_{\text{nmo}}(0)$  and  $\eta$  using two distinctly different dips (Alkhalifah and Tsvankin, 1995). The results of this inversion, to be refined after the resampling procedure, make it possible to reduce the range of both parameters used in the 2-D scan.

Our synthetic and field-data examples show that the standard isotropic Fowler method cannot handle general (nonelliptical) transversely isotropic media. While it is feasible to find an isotropic velocity that images one or two dipping events well, it is practically impossible to image a wide range of dips without taking anisotropy into account.

In contrast, the anisotropic Fowler algorithm, based on the equations for transverse isotropy, enables us not only to obtain a good-quality image, but also to recover the correct values of the parameters  $V_{\text{nmo}}(0)$  and  $\eta$ . In our synthetic example, we have generated and analyzed many other  $V_{\text{nmo}}(0)$  and  $\eta$  panels that could not be shown here. We observed some degree of trade-off between the two coefficients, but the correct pair of  $V_{\text{nmo}}(0)$  and  $\eta$  produces by far the best-quality overall image for a wide range of dips. Although we have been able to improve the quality of fault-plane imaging in our case study, future work is necessary to demonstrate how successful this method can be as a way for estimating anisotropic parameters. For instance, the influence of spatial variations in the medium parameters on the DMO-migration sequence deserves a separate study.

Our algorithm is based on the hyperbolic moveout equation and, in principle, can lead to errors on long spreads because of the anisotropy-induced nonhyperbolic moveout (Tsvankin and Thomsen, 1994). However, the magnitude of nonhyperbolic moveout for typical transversely isotropic media becomes smaller at steep dips (Tsvankin, 1995). The results in Anderson

and Tsvankin (1994) demonstrate that the hyperbolic moveout equation for VTI media remains accurate up to surprisingly large offsets at steep dips, if the correct NMO velocity is used.

To use the output of the Fowler DMO algorithm in poststack migration, we have also extended Stolt  $F$ - $K$  migration algorithm to transverse isotropy. On the whole, the Fowler-type DMO method, along with the parameter-estimation procedure and Stolt poststack migration, represents a full-scale processing system for transversely isotropic media with arbitrary strength of the anisotropy. In the future, it may be possible to extend these results to more complex anisotropic models (e.g., orthorhombic) since the analytic NMO equation used here can be applied in symmetry planes of any anisotropic medium.

#### ACKNOWLEDGMENTS

John Toldi and Chris Dale (Chevron Overseas Petroleum, Inc.) identified anisotropy in a survey from offshore Africa and provided the data to the Center for Wave Phenomena for the testing of newly developed anisotropic codes. Tagir Galikeev (CSM) did the preprocessing on the field data set. We are grateful to Ken Larner (CSM), Omar Uzcatogui (CSM) and Denis Schmitt (Mobil) for helpful discussions and suggestions. Comments made by the reviewers helped to improve the paper. This work was performed during J. Anderson's tenure as Mobil Visiting Scientist in the Department of Geophysics at the Colorado School of Mines. I. Tsvankin acknowledges the support provided by the members of the Consortium Project on Seismic Inverse Methods for Complex Structures at the Center for Wave Phenomena, Colorado School of Mines, and by the United States Department of Energy, Grant Number DE-FG02-89ER14079 (this support does not constitute an endorsement by DOE of the views expressed in this paper). T. Alkhalifah was supported by KACST, Saudi Arabia.

#### REFERENCES

- Alkhalifah, T., 1995, Efficient synthetic-seismogram generation in transversely isotropic, inhomogeneous media: *Geophysics*, **60**, 1139–1150.
- Alkhalifah, T., and Tsvankin, I., 1995, Velocity analysis for transversely isotropic media: *Geophysics*, **60**, 1550–1566.
- Anderson, J., and Tsvankin, I., 1994, Dip-moveout processing by Fourier transform in anisotropic media: 64 Ann. Internat. Mtg., Soc. Expl. Geophys., Expanded Abstracts, 1213–1216.
- Dellinger, J. A., 1991, Anisotropic wave propagation: Ph.D. thesis, Stanford University.
- Fowler, P., 1984, Velocity independent imaging of seismic reflectors: 54th Ann. Internat. Mtg., Soc. Expl. Geophys., Expanded Abstracts, 383–385.
- , 1988, Seismic velocity estimation using prestack time migration: Ph.D. thesis, Stanford University.
- Hale, D., 1991, Dip moveout processing: SEG Course Notes, Volume 4.
- Hale, D., and Artley, C., 1993, Squeezing dip moveout for depth-variable velocity: *Geophysics*, **58**, 257–264.
- Helbig, K., 1983, Elliptical anisotropy—its significance and meaning: *Geophysics*, **48**, 825–832.
- Kitchenside, P., 1991, Phase shift-based migration for transverse isotropy: 61st Ann. Internat. Mtg., Soc. Expl. Geophys., Expanded Abstracts, 993–996.
- Levin, F. K., 1971, Apparent velocity from dipping interface reflections: *Geophysics*, **36**, 510–516.
- Stolt, R. H., 1978, Migration by Fourier transform: *Geophysics*, **43**, 23–48.
- Thomsen, L., 1986, Weak elastic anisotropy: *Geophysics*, **51**, 1954–1966.
- Tsvankin, I., 1995, Normal moveout from dipping reflectors in anisotropic media: *Geophysics*, **60**, 268–284.
- , 1996,  $P$ -wave signatures and notation for transversely isotropic media: An overview: *Geophysics*, **61**, 467–483.
- Tsvankin, I., and Thomsen, L., 1994, Nonhyperbolic reflection moveout in anisotropic media: *Geophysics*, **59**, 1290–1304.
- Uren, N. F., Gardner, G. N. F., and McDonald, J. A., 1990, Normal moveout in anisotropic media: *Geophysics*, **55**, 1634–1636.